Available online at www.sciencedirect.com
SCIENCE DIRECT®
Journal of Chromatography A, 1082 (2005) 33–42
JOURNAL OF CHROMATOGRAPHY A
www.elsevier.com/locate/chroma

On-line identification of secondary metabolites in freshwater microalgae and cyanobacteria by combined liquid chromatography–photodiode array detection-mass spectrometric techniques

Rita Frassanito [a], Marco Cantonati [b], Massimiliano Tardìo [b], Ines Mancini [a], Graziano Guella [a,*]

[a] *Bioorganic Chemistry Laboratory, Department of Physics, University of Trento, Via Sommarive 14, I-38050 Povo, Trento, Italy*
[b] *Limnology & Phycology Section, Museo Tridentino di Scienze Naturali, Via Calepina 14, I-38100 Trento, Italy*

Available online 8 March 2005

Abstract

The analysis and identification of a wide range of secondary metabolites biosynthesized by different algal taxa and cyanobacteria has been performed through a selective and sensitive methodology, mainly based on reversed-phase HPLC coupled both to UV photodiode array detection and to atmospheric pressure mass spectrometric techniques (HPLC–DAD-APIMS). Results are reported here with special attention to the analyses carried out both on the natural phytoplankton (mixed populations) of Lake Tovel (Northern Italy, Brenta Dolomites) and on enclosure-produced biomass of the dinoflagellate *Glenodinium sanguineum* Marchesoni (1941). This analytical procedure might represent a powerful tool for the fast screening of the taxonomic composition (broad groups, e.g. divisions) of natural mixed populations of phytoplankton, by providing a reliable distribution of accessory pigments extracted from microalgae, such as carotenoids and chlorophyll derivatives. Furthermore, we showed that in the same chromatographic analysis other classes of natural products, such as galactolipids, alkaloids, sterols and mycosporine-like amino acids, can be detected by using combined optical and mass spectrometric techniques. These metabolites represent distinctive biochemical signatures, sometimes even at the species level.

Keywords: Phytoplankton; Microphytobenthos; Chemotaxonomy; LC–MS; Pigments; MAAs; Galactolipids

1. Introduction

Phytoplankton and phytobenthos microalgae and cyanobacteria are major primary producers in aquatic ecosystems. These photoautotrophs grow in response to a complex interplay of physical and chemical factors and provide the basis of biological productivity in these systems. Two complementary approaches to measuring phytoplankton distribution and composition are increasingly used. Whereas the first faces the problem of phytoplankton and phytobenthos quantification by means microscopical analyses [1–3] (identifications, counts, measurements and biovolume calculations), the second method relies on analyses of carotenoid and chlorophyll pigments by HPLC coupled to photodiode array detector (DAD) [4]. This latter approach can provide valuable cross-validating information, since pigment data can be used to characterise the broad algal classes that may be present in a given sample [5]. However, a number of difficulties limit the application of the HPLC-DAD approach both in the determination of algal division composition [6] and in the unambiguous identification of all the pigments present in a given biological extract. In fact, due to the high number of known carotenoids (more than 600 different structures have so far been isolated from natural sources [7]) and to their similar electronic structure, a significant number of carotenoids show undistinguishable UV–vis spectra. In order to overcome these difficulties,

* Corresponding author. Tel.: +39 0461 881536; fax: +39 0461 882009.
E-mail address: graziano.guella@unitn.it (G. Guella).

0021-9673/$ – see front matter © 2005 Elsevier B.V. All rights reserved.
doi:10.1016/j.chroma.2005.02.066

atmospheric pressure mass spectrometry coupled to liquid chromatography (LC–APIMS) has been introduced [8] exploiting the great performances of electrospray (ESI) and chemical ionization (APCI) soft ion sources.

Whatever the analytical technique used to tackle the problem, the basis of this chemical approach relies on the evidence that some pigments are very specific to a microalgal taxa (mostly divisions) and, hence, that they could be used as a biochemical "signature" of the algal assemblage composition [5]. It is now becoming more and more evident, however, that pigment analysis is per se not at all sufficient for a full assessment of phytoplankton or phytobenthos biodiversity. In fact, some pigments which are prominent in one division (e.g. fucoxanthin in diatoms) can sometimes be found in other ones (chrysophythes in the case of fucoxanthin); moreover, their production can vary depending on the physiological status of algae and/or on environmental factors, stress level and nutrition [9,10]. The consequence is that, even if pigment analysis has been claimed for many years to represent a powerful tool in taxonomy and in quali-/quantitative estimations, it suffers of difficulties in both targets. While we have already mentioned the reasons for the latter, it should be also noted that phytoplankton or phytobenthos taxonomy by means of pigment analysis cannot be done at a low rank (species or genus level) since phylogenetic differences, determining also diversity in structural pigments, become significant only at higher levels (classes, divisions) [5–6]. It follows that, without using the taxonomic information provided by microscopic analyses at the genus/species level, HPLC (and CHEMTAX) analyses would produce important errors in the taxonomic identification. To this regard, the example supplied by the unique biomarker of the dinoflagellate *Karenia brevis*, the carotenoid gyroxanthin-diester [11], is paradigmatic.

Other secondary metabolites, such as polyketides, alkaloids, lipids, terpenes, sterols and modified amino acids would be better biochemical "species signatures", since they are usually produced only by some species of a genus (sometimes their biosynthesis is even strain specific) and few of them have been so far isolated in more than one species [12–13]. Their chemical identification is not, however, as straightforward as pigment analysis, because they could escape UV–vis detection (due to their intrinsically low UV response factor) and, more importantly, their unusual chemical features need a more complex approach for the structure elucidation, mainly relying on heavy and expensive NMR methodologies. The aim of this paper is to propose an integrated approach based on reversed-phase HPLC–DAD-APIMS techniques which is suitable for the analysis and identification of a wide number of specific taxonomic markers present in a given algal species, in a mixed phytoplankton or in a phytobenthos sample.

We will demonstrate that, in the same chromatographic run optimized for pigment detection, other classes of metabolites (here mycosporine-like amino acids, sterols and galactolipids) can be identified by on-line LC–ESI-MS techniques. In particular, we will report the results of our analysis of the main secondary metabolites of natural phytoplankton samples of Lake Tovel (Brenta Dolomites, Northern Italy), of enclosure-produced biomass [14] of the dinoflagellate *Glenodinium sanguineum* Marchesoni (1941) and of a microphytobenthos sample of the same lake. Lake Tovel became rather famous because of spectacular and regular summer red blooms, which however ceased in 1964. These red blooms were due to a dinoflagellate species characterized by important amounts of a red carotenoid in the cytoplasm and was described by Marchesoni as *Glenodinium sanguineum* in 1941. Baldi (1941) studied in detail the reddening phenomenon and distinguished red and green forms, hypothesising that the red forms derived from the green ones by means of light induced massive carotenoid synthesis. Recent evidences have shown that the two forms belong in reality to two different species and even genera [15–16]. While the taxonomy of the two new forms is being clarified and established, we will continue referring to this dinoflagellate as *Glenodinium sanguineum*, naming *Gs*-green and *Gs*-red, the green and the red species, respectively.

2. Experimental

2.1. Materials

All the used solvents were of analytical grade (Merck, Darmstadt, Germany) or HPLC grade (Riedel deHaen, Sigma Chemical Co., St. Louis, MO, USA). Ammonium acetate was purchased from Merck.

All evaporations were carried out at r.t. under reduced pressure. Reversed phase flash chromatography (FC) was performed with Merck LiChroprep RP–18 (40–63 μm).

2.2. Field samples

The samples used for chemical and microscopical analyses were collected using different approaches.

2.2.1. Sample A (Gs-green)

Sample A (*Gs*-green) collected by means of a water pump from the margins of a cylindrical enclosure positioned in Lake Tovel during summer 2002, where green-orange dinoflagellate aggregates were observable; aggregates were obtained adding algal nutrients (P and N) to the experimental structures (enclosures or mesocosms) [14]. In this sample the species *Gs*-green was dominant (reaching a biovolume of $11.3\,mm^3\,l^{-1}$); the sole other species present was *Fragilaria tenera* with a biovolume of about $1.4\,mm^3\,l^{-1}$.

2.2.2. Sample B (Gs-green cysts)

Sample B (*Gs*-green cysts) collected from the bottom of little aquaria inside which the green-orange dinoflagellate aggregates mentioned above deposited after encystment. They were obtained simply by preserving the aquaria exposed to daylight at a room temperature of 20–25 °C for some weeks.

This sample contained exclusively high densities of *Gs*-green cysts.

2.2.3. Sample C (horizontal phytoplankton net tow)

Sample C (horizontal phytoplankton net tow) collected from the first 2 m of the open water of Lake Tovel in the beginning of summer 2003 by means of a phytoplankton sinusoidal net-tow (mesh-size = 10 μm). Here the dominant species were planktonic diatoms (*Cyclotella* spp.) reaching biovolumes of about 0.4 $mm^3 l^{-1}$. Three dinoflagellates species were present: *Gymnodinium uberrimum* (about 0.12 $mm^3 l^{-1}$) and both *Gs*-green and *Gs*-red morphospecies (total biovolume of about 0.09 $mm^3 l^{-1}$; *Gs*-red/*Gs*-green ratio of about 0.05).

2.2.4. Sample D (vertical phytoplankton net tow)

Sample D (vertical phytoplankton net tow) collected from the deepest point of Lake Tovel (maximum depth = 39 m) in autumn 2003 by means of the same phytoplankton net mentioned above. The upper 30 m were sampled by means of a vertical net haul. The dominant taxa were the chrysophyta *Uroglena* sp. (biovolume of about 1.4 $mm^3 l^{-1}$) and the dinoflagellate *Gymnodinium uberrimum* (about 1.1 $mm^3 l^{-1}$). *Gs*-green maintained at biovolume of about 0.2 $mm^3 l^{-1}$.

2.2.5. Sample E (stone microphytobenthos)

To study stone-dwelling (epilithic) cyanobacteria, stones were taken by divers at different depths along a profile (0.5, 3, 6, 9, 12, 15, 18, 21 and 24 m). Coverages were removed with a toothbrush on known surfaces delimited by a template to obtain quantitative samples. Besides a number of diatom taxa, the sample here investigated (0.5 m) was dominated by cyanobacteria, the most common genera at increasing depths being *Calothrix*, *Scytonema*, *Schizothrix*, *Ammatoidea*, *Tolypothrix* and *Geitleribactron*.

Counts were carried out using an OLYMPUS IX70 and IX71 inverted microscope according to Utermöhl [3]. At each magnification, at least 100 individuals of the dominant taxon were counted, which corresponds to an error of about 20% [1]. Algal biovolume was calculated from linear dimensions according to Rott [2]. A part of the samples collected were preserved with Lugol's solution acidified with 10% of CH_3COOH for phytoplankton biovolumes determination; the remaining part were filtered in the field within a few hours on Whatman GF/C 0.45 μm filters, which were then stored at −20 °C until extraction for chemical analyses.

The sample ($\sim 10^5$ cells) were extracted (two times) both by of 100% HPLC-grade acetone (3 ml) and by methanol (two times, 3 ml). The extraction procedure was repeated until filter decoloration, the extracted were combined, reduced to dryness by rotary evaporation, redissolved in 500 μl of acetone/methanol 1:1 and stored in ambered glass vials under nitrogen until analysis. The injected volume of any sample was 10 μl.

2.3. Instruments

LC–MS and LC–MS–MS was performed on a Hewlett-Packard Model 1100 Series liquid chromatograph coupled both to a PDA (Photo Diode-Array) detector (Agilent 1100 Series) and to a Bruker Esquire-LC quadrupole ion trap mass spectrometer equipped with atmospheric pressure ESI and APCI interfaces. A Rheodyne 7725 (Cotati, CA, U.S.A.) injection valve equipped with a 20 μl internal loop was used for the injections.

2.4. HPLC–APIMS and MS–MS on the raw extracts

The PDA was set at the wavelength of 215, 450 and 665 nm, and all the spectra were recorded.

The analyses were carried out at room temperature on an Agilent ZORBAX Eclipse XDB-C8 150 × 4.6 mm, 3.5 μm. The eluent (0.8 ml/min) consisted of (A) methanol/28 mM ammonium acetate (70:30) and (B) methanol, using a linear gradient: 35–100% of B in 40 min, and the isocratic methanol 100% was held 10 min. Then the initial conditions of mobile phase were reached in 20 min.

A 7:3 split of the column effluent was used to achieve a flow rate of 240 μl/min into the mass spectrometer. High-purity nitrogen was used as nebulizer and dry gas. The nitrogen dry gas was at a constant flow rate of 6 l/min, heated to 300 °C. Further parameters during LC–MS analyses were: trap drive 54, skim 1 set at −43.2 V in negative mode and trap drive 44, skim 1 set at 43.2 V in positive mode.

2.4.1. ESI

The capillary in the ESI interface was set at a voltage of 4000 V and the nebulizer gas pressure was 20 psi.

2.4.2. APCI

The HV corona was set at 1700 V, the nebulizer gas pressure was 30 psi and the APCI source temperature 450 °C.

2.4.3. MS–MS of galactolipids

Collisionally activated dissociation (CAD) was performed by on-line positive-ion ESI-MS on the $[M + Na]^+$ ions as described previously [17].

2.5. HPLC–ESI-MS of MAAs

Crude extracts obtained from standard work-up were partially purified by reversed-phase flash chromatography (CH_3CN/MeOH gradient elution). The first fraction (sample A1), which contains the most polar compounds, was further analysed by setting PDA wavelength at 320 nm. The analysis on sample A1 was carried out at room temperature on Merck RP-18 Lichrosphere 240 × 4.6 mm, 5 μm; eluent: HCOOH 1%, 1 min, gradient 0–100 % CH_3OH + HCOOH 1% in 30 min, 1 ml/min.

A 7:3 split of the column effluent was used to achieve a flow rate of 300 μl/min into the ESI source, operating in

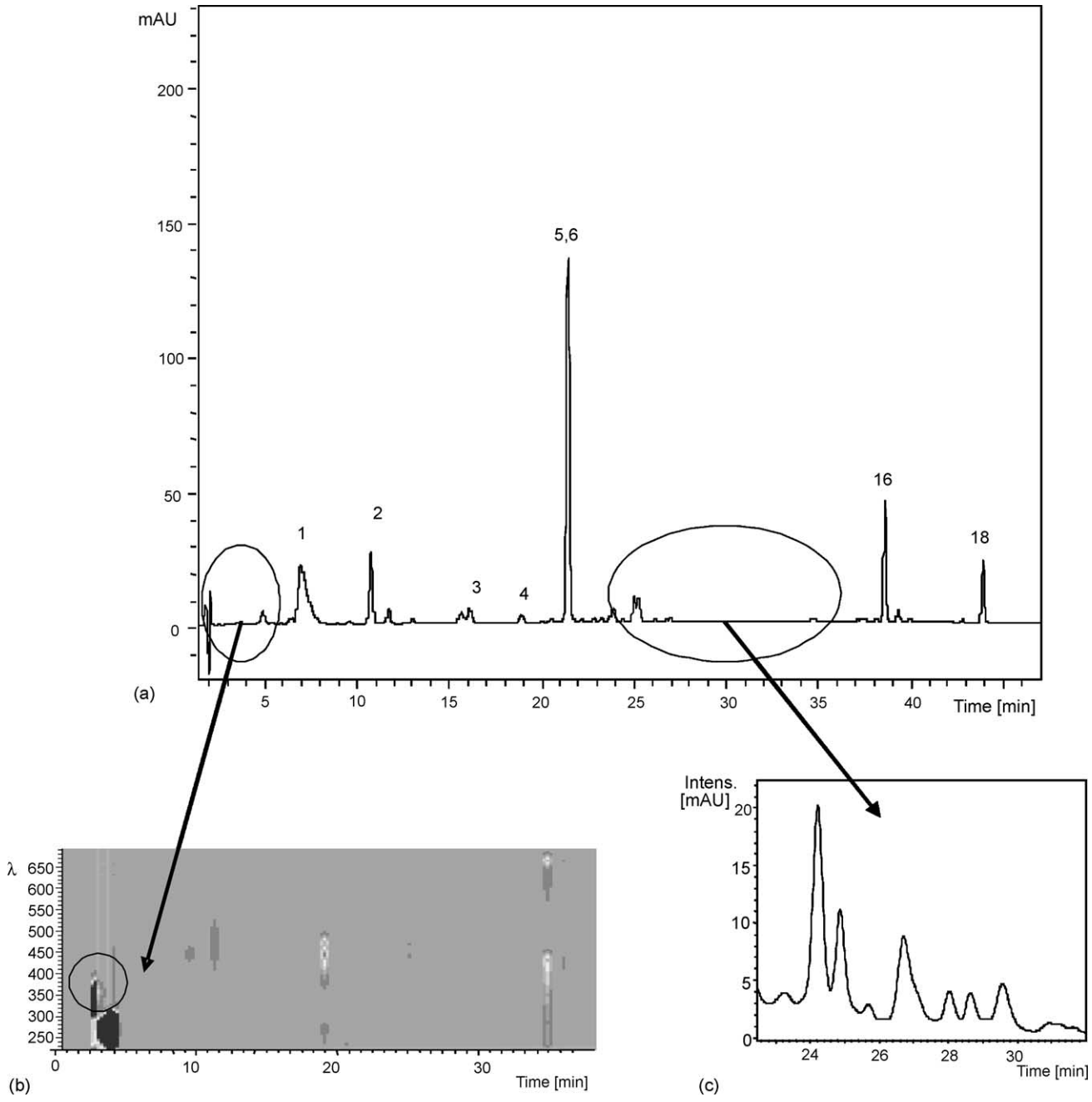

Fig. 1. HPLC–DAD-APIMS analysis of the main secondary metabolites of the motile cells of *Gs*-green (sample A) from the enclosures of the Lake Tovel obtained by the linear gradient H_2O/CH_3OH containing $NH_4C_2H_3O_2$. Carotenoids and chlorophylls are recorded at 450 nm (a) and assigned in Table 1; the plot of iso-absorbance (b) points out the strong absorption between 300–400 nm of mycosporine-like aminoacids in the first minutes; the galactolipid profile at 215 nm (c) can be fully spread out by on-line negative- and positive-ion mode ESI-MS and ESI-MS–MS (Table 2).

positive-ion mode. High-purity nitrogen was used as nebulizer and dry gas. The nitrogen dry gas was at a constant flow rate of 8 l/min, heated to 350 °C.

The capillary in the ESI interface was set at a voltage of 4000 V and the nebulizer gas pressure was 25 psi. Further parameters during LC–MS analyses were: trap drive 41.6, skim 1 set at 28.9 V.

2.6. NMR measurements

^{1}H NMR experiments were performed with a Varian XL-300 or with Bruker Advance spectrometer operating at 300 MHz and 400 MHz, respectively. ^{1}H NMR spectra were taken at 298 K in $CDCl_3$ (δ_H 7.25 ppm) for pigments, in CD_3OD (δ_H 3.31 ppm) for galactolipids

and in D_2O (δ_H 4.72 ppm) for mycosporine-like amino acids.

3. Result and discussion

The raw extracts of sample A and B (*Gs*-green motile cells and *Gs*-green cysts, respectively) and of the natural phytoplankton (samples C, D) and microphytobenthos (sample E) communities of Lake Tovel have been analysed by reversed-phase RP-8 column with a gradient elution system consisting of methanol-28 mM ammonium acetate in water, photodiode-array detection and different MS experimental set-up (negative- or positive-ion mode, ESI or APCI ionisation, full scan or MS–MS). Analyses have been focused on four classes of metabolites: pigments, mycosporine-like amino acids, galactolipids and sterols.

3.1. Pigments

Fig. 1 shows the HPLC–DAD-APIMS analysis of a raw extract of the motile cells (sample A) of *Gs*-green, which has been demonstrated by microscopic analysis to be the largely prevalent dinoflagellate of the mesocosms. The chromatogram at 450 nm (Fig. 1a) displays an apparently good separation of pigments and the corresponding UV–vis spectra of each chromatographic peak seem to allow an unambiguous assignment of each pigment (Table 1). However, even if the major peak at t_R 23 min shows an UV–vis spectrum attributable to pure diadinoxanthin by DAD peak purity software, the corresponding full-scan mass spectra (taken either by ESI or APCI) speak for the presence of two co-eluting compounds, diadinoxanthin and dinoxanthin. In particular, by APCI-MS it is even possible to establish their relative

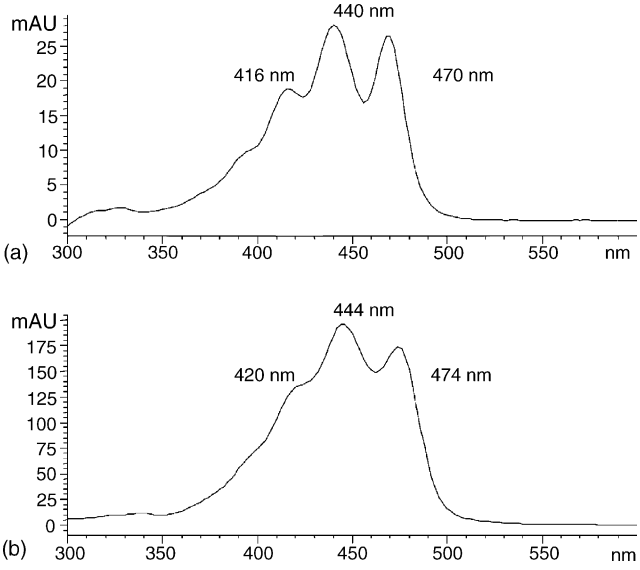

Fig. 2. On-line UV–vis spectra of dinoxanthin (a) and diadinoxanthin (b) as obtained by HPLC-DAD analysis of the raw extracts of *Gs*-green (sample A), using the same eluent of Fig. 1 but a different column (Merck RP-18 Lichrosphere 240 × 4.6 mm, 5 μm).

weight (diadinox/dinox ∼11) as the ratio between the areas of the corresponding relevant ions. In fact, APCI spectrum of diadinoxanthin shows $[M + H]^+$ at *m/z* 583 and its fragment-ion $[M + H–H_2O]^+$ at *m/z* 565, whereas for dinoxanthin corresponding ions at *m/z* 643 and *m/z* 625 can be detected. The failure of their distinction by DAD analysis can be easily explained taking into account the strong resemblance of their visible spectra (Fig. 2). The presence of peridinin, diadinoxanthin and β-carotene in the raw extract of *Gs*-green has been ascertained by off-line NMR measurements. After extensive chromatographic purification of a massive collection

Table 1
Pigment composition of the investigated samples by HPLC–DAD-APIMS analysis

	Pigment	Main UV–vis absorption bands (nm)	ESI + (*m/z*)	APCI + (*m/z*)	Sample
1	Chlorophyll *c*2, *c*3	446, 634	609, 611		A, B, C, D
2	Peridinin	474	653	631, 613, **553**	A, B, C, D
3	Fucoxanthin	450	681	659, **641**	A, C, D
4	Astaxanthin	478	619	597	A, B, C, D
5	Dinoxanthin	416, 440, 470	665	643, **625**	A, B, C, D
6	Diadinoxanthin	420, 444, 474	605	**583**, 565	A, B, C, D
7	Adonirubin	[a]	603		B
8	Unknown	418, 440, 468	605		C
9	Astaxanthin diacetate	[a]	703		B
10	Zeaxanthin	420, 444, 472	591		B, C, D
11	Adonirubin acetate	470	645		B
12	Cantaxanthin	476	589		B, D
13	Astacene	470	615		B
14	Chlorophyll *b*	468, 652	906		D
15	Adonirubin monoester 22:5	470	915, **893**		B
16	Chlorophyll *a*	432, 665	892		A, B, C, D
17	Adonirubin monoester 18:4	470	**861**, 839		B
18	β-Carotene	424, 450, 476		537	A, B, C, D

The peaks with the major relative abundance are in bold. (A) Motile cells of *Gs*-green in the enclosure, (B) resting cells of *Gs*-green, (C) horizontal net tow sample, (D) vertical net tow sample.
[a] Overlapped chromatographic peaks.

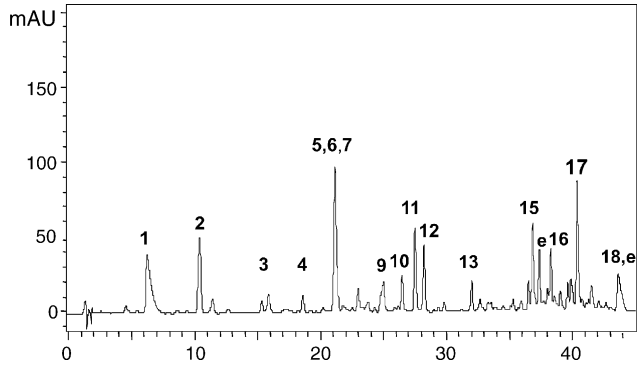

Fig. 3. UV–vis chromatogram at 450 nm corresponding to the RP-8-HPLC–DAD pigment analysis of the resting cells (sample B) of *Gs*-green. The peaks were identified (Table 1) by UV–vis spectra and positive-ion mode ESI-MS spectra.

($\sim 10^7$ cells) of motile cells as obtained by an induced bloom of this species, ^{1}H NMR spectra were taken on pure samples of these carotenoids confirming the exactness of the assignments in Table 1.

It is worth mentioning that, whereas a very low amount of astaxanthin has been always detected in all the samples of dinoflagellate aggregates (induced blooms), it is significantly more abundant in the raw extract of the resting cysts (sample B) of the same dinoflagellate (Fig. 3 and Table 1). Actually, the chromatogram of this sample shows a general higher complexity than that previously discussed. ESI-MS data establish that (i) the peak at t_R 21.5 min, assigned to diadinoxanthin and dinoxanthin in sample A, contains here also adonirubin and (ii) other putative precursors of astaxanthin, such as adonirubin acetate, cantaxanthin and adonirubin esters are also present. This outcome demonstrates that the biosynthesis of carotenoids in *Gs*-green is strongly dependent from its life-cycle stage: in particular, our analysis has clearly shown that during encystment a complex series of enzymatic oxidations (possibly initiated by the introduction of a keto function at C4 on β-carotene [18]) and esterifications must work. Only the biochemical analyses of related enzymes and through study of the intermediate metabolism will allow the routes of astaxanthin biosynthesis in this microrganism to be exactly determined.

In order to ascertain that in situ induced microalgal bloom contains motile cells belonging to a single morphospecies (*Gs*-green), we have analyzed the pigment distribution in a horizontal net tow (sample C, Fig. 4a), and in a vertical net tow sample (sample B, Fig. 4b) and the results of our assignments are reported in Table 1. By microscopic examination of these samples, the biovolume of all the dinoflagellates present in the sample D was estimated to be about 50% and the contribution of *Gs*-green about 7%, whereas the sample C contained dinoflagellates as much as 35% where *Gs*-green was estimated to be 14% and *Gs*-red 0.7%. This is somehow reflected in the corresponding chromatographic profiles showed in Fig. 4 wherein a wider pigment composition with respect to sample A can be appreciated.

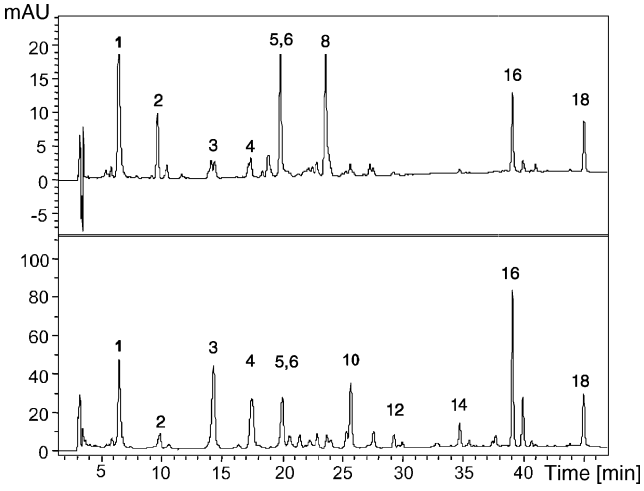

Fig. 4. Pigment analysis at 450 nm of raw algal extracts from a horizontal net tow sample (sample C), and from a vertical net tow sample (sample D) under experimental conditions used in Figs. 1 and 3. For chromatographic peak identification see Table 1.

3.2. *Mycosporine-like amino acids*

MAAs are water-soluble substances characterized by a cyclohexenone or cyclohexenimine chromophore conjugated with the nitrogen substituent of an amino acid or its imino alcohol, having absorption maxima ranging from 310 to 360 nm and an average molecular weight of around 300 [19]. The plot of iso-absorbance of the HPLC–DAD-APIMS analysis of sample A (Fig. 1b) reveals a class of very polar compounds, eluting in the first minutes of the chromatographic run and showing a strong absorption around 350 nm. By changing the mobile phase composition, this fraction can be resolved in three major components, which can be preliminarily identified as mycosporine-like aminoacids (MAAs) by on-line LC–MS experiments. The major compounds have been identified as palythine and palythene [20] eluting at t_R 3.6 and at t_R 10.2 min, respectively, in the chromatographic conditions of Fig. 5. The structures were initially guessed by their characteristic UV spectra and then confirmed by positive-ion ESI full scan mass spectra whereby $[M + H]^+$ ion of palythine was detected at *m/z* 245 and $[M + H]^+$ ion of palythene at *m/z* 285. The major compound contained in the unresolved peak at t_R = 8.4–8.7 min was detected as $[M + H]^+$ at *m/z* = 260 and belongs to mycosporine–alanine. ^{1}H NMR measurements carried out on purified fraction of this sample were actually found in agreement with LC–MS outcome.

3.3. *Galactolipids*

Lipids are integral components of thylakoid membranes and fundamental parts for the structural and functional integrity of the photosynthetic apparatus and galactolipids are the predominant lipids of photosynthetic membranes. In these natural compounds the galactopyranose moiety is linked to the glycerol backbone bearing two long hydrocarbon chains

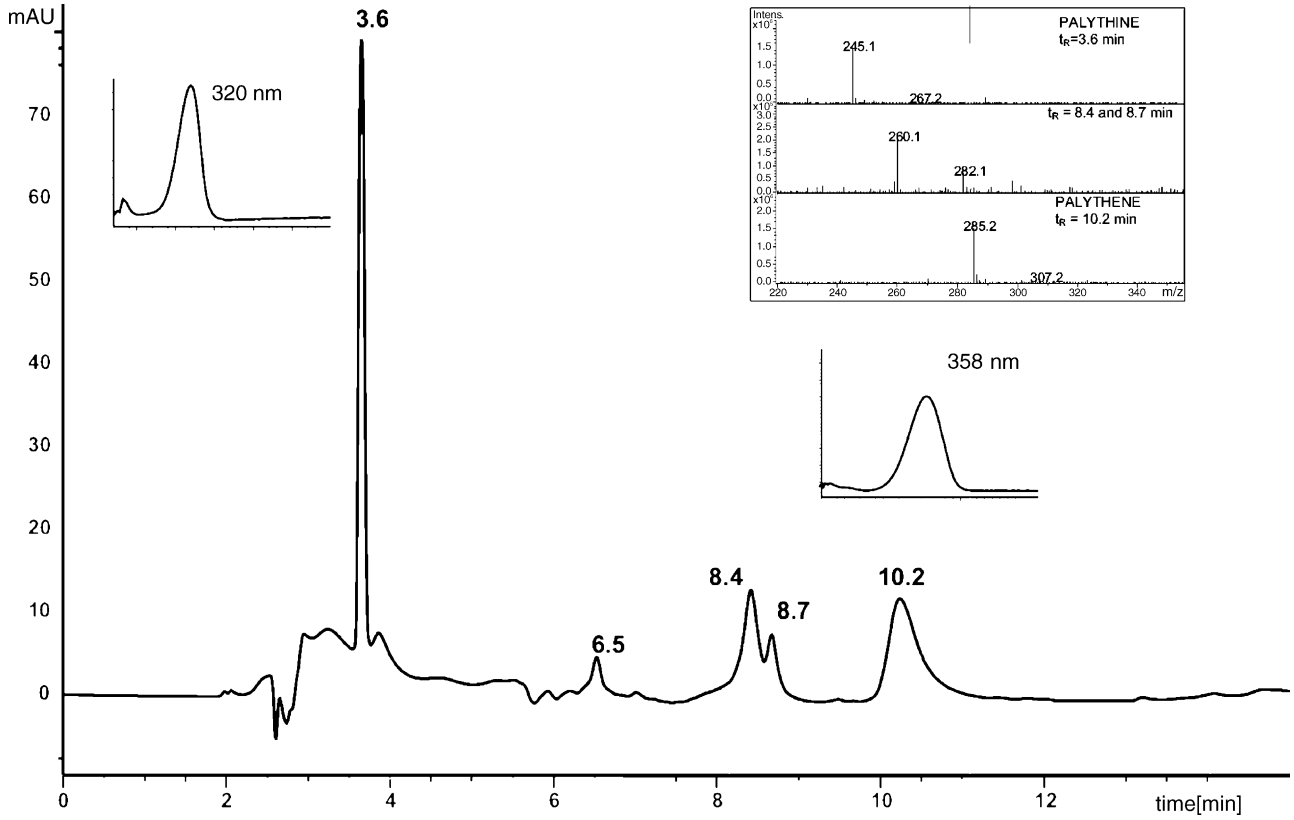

Fig. 5. Analysis of MAAs in a partially purified fraction of cellular extract of *Gs*-green (sample A1). Chromatogram recorded at 320 nm by H_2O/CH_3OH gradient containing HCOOH with Merck RP-18 Lichrosphere column 240 × 4.6 mm, 5 μm. UV spectra of palythine and palythene at t_R = 3.6 and 10.2 min, respectively. In the top-right region, the positive-ion mode ESI-MS spectra of the main compounds are also shown.

Table 2
Monogalactolipids (MGDG) and digalactolipids (DGDG) as detected on sample A by on-line negative- and positive-ion mode ESI-MS and ESI-MS–MS

Compound	Formula	$[M–H]^-$	$[M+Na]^+$	Fatty acid composition	Abundance%
MGDG	$C_{41}H_{70}O_{10}$	721	745	18:4/14:0	[a]
	$C_{43}H_{68}O_{10}$	743	767	18:3/16:4	[a]
	$C_{45}H_{66}O_{10}$	765	789	18:5/18:5	16.1
	$C_{45}H_{68}O_{10}$	767	791	18:5/18:4	20.7
	$C_{45}H_{70}O_{10}$	769	793	18:4/18:4	6.0
	$C_{45}H_{72}O_{10}$	771	795	18:4/18:3	[a]
	$C_{45}H_{74}O_{10}$	773	797	18:2/18:4	[a]
	$C_{47}H_{70}O_{10}$	793	817	20:5/18:5	6.2
	$C_{47}H_{72}O_{10}$	795	819	20:5/18:4	[a]
DGDG	$C_{47}H_{80}O_{15}$	883	907	18:4/14:0	[a]
	$C_{51}H_{76}O_{15}$	927	951	18:5/18:5	[a]
	$C_{51}H_{78}O_{15}$	929	953	18:5/18:4	7.3
	$C_{51}H_{80}O_{15}$	931	955	18:4/18:4	33.7
	$C_{51}H_{82}O_{15}$	933	957	18:3/18:4	[a]
	$C_{53}H_{82}O_{15}$	957	981	20:5/18:4	[a]
	$C_{55}H_{84}O_{15}$	983	1007	20:5/20:5	[a]

The percent abundance is calculated by integration of UV traces at 215 nm.
[a] Estimated to be about 1%.

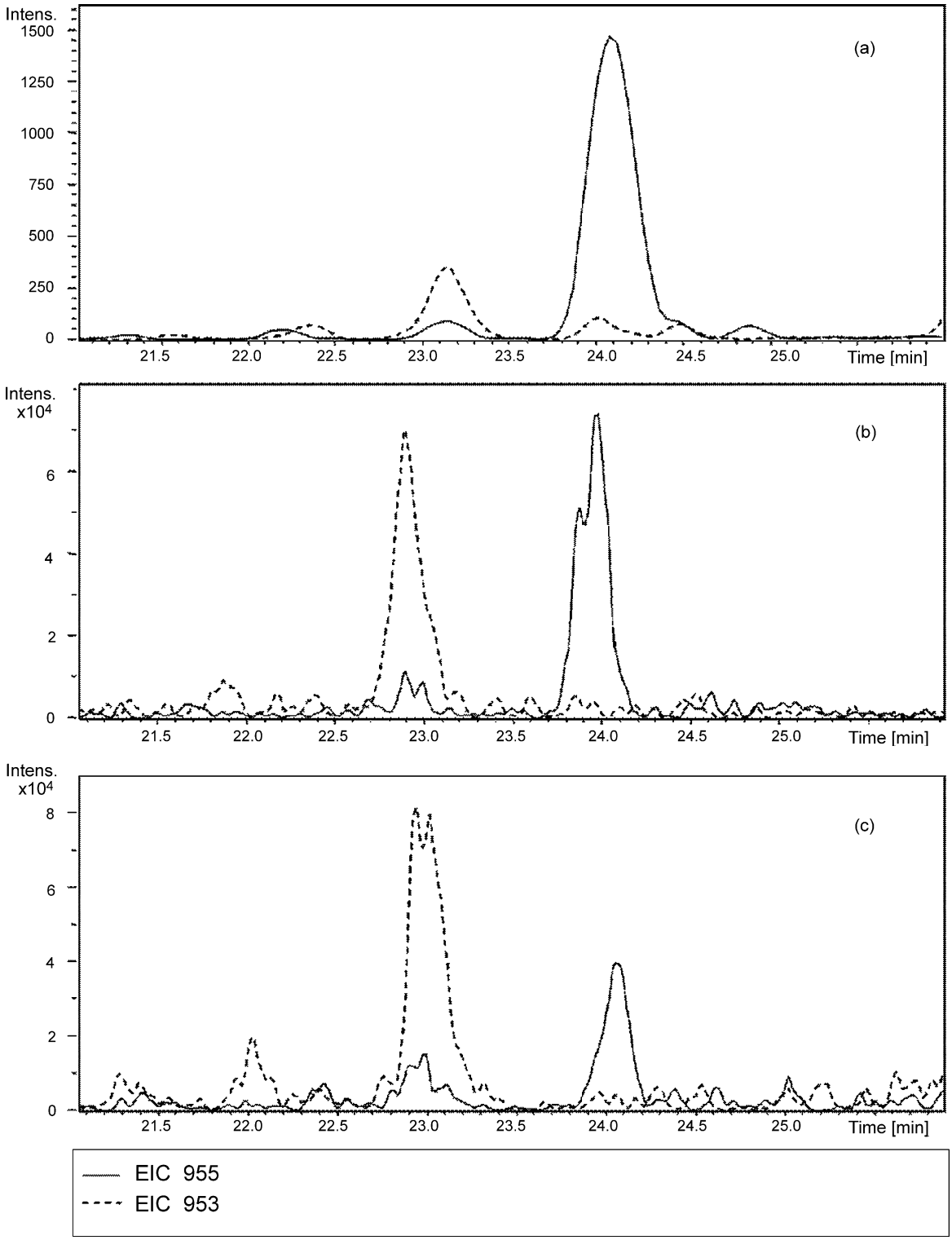

Fig. 6. Ion-extracted traces of the $[M + Na]^+$ ions of the DGDG 18:4/18:4 (—) at *m*/*z* 955 and 18:5/18:4 (- -) at *m*/*z* 953 respectively in different samples (a) in the sample A (DGDG 18:4/18:4 as major); (b) in the sample C (DGDG 18:4/18:4 and DGDG 18:5/18:4 in comparable amount); and (c) in the sample D (DGDG 18:5/18:4 as major).

and the more representative substances are the monogalactosyldiacylglicerols (MGDG) and the digalactosyldiacylglycerols (DGDG). Specific roles played by these compounds in the light reactions of photosynthesis justify considerable interest for their bioactivity (in particular when the acyl chains are polyunsaturated) and potential use as chemotaxonomic markers has led to increasing attention toward this class of natural products [21].

These lipids can be revealed either by short wavelength (215 nm) UV-DAD or by ESI-MS detection in the same chromatographic run used for the pigments detection as shown in Fig. 1c (eluting between 23 and 35 min). The determination of β-galactopyranose moiety, the geometrical configuration of the double bounds and their actual position in the fatty chains (ω-3 or ω-6) has been assessed by ^{1}H NMR spectroscopic analysis on the partially purified compounds (data not shown).

The ESI mass spectra allow the molecular mass determination, producing both high $[M–H]^-$ ions by negative-ion, and $[M + Na]^+$ ions by positive-ion, and structural information concerning the fatty acid composition by the in-source CID fragments. Moreover, the on-line fragmentation of $[M + Na]^+$ ions by positive-ion ESI-MS–MS allowed us to establish the positional distribution of the *sn*-glycerol-bound fatty acyl chains [17]. The overall results of our galactolipid analysis of sample A are reported in Table 2. A complex mixture of digalactolipids DGDG and their corresponding monogalactolipids MGDG has been assessed here. Moreover, by our analysis a rough estimation of their relative amount can be found by integration of their UV peak-area as detected at 215 nm assuming identical extinction coefficients. Within this approximation, we have found that the digalactolipid, displaying $[M + Na]^+$ pseudo-molecular ion at *m*/*z* 955, bears identical fatty acyl chains (octadeca–tetraenoyl, 18:4) on the glycerol backbone, as established by tandem MS experiments, and is the most abundant of all the galactolipids in the sample A.

Whereas the pigment distribution of *Gs*-green encysted cells (sample B) is very different from that of its motile cells (sample A), our LC–tandem MS measurements show that even during encystment the most representative galactolipid remains the DGDG with 18:4/18:4 fatty chains (data not shown).

Fig. 6 shows the comparison between the ion-extracted traces due to the $[M + Na]^+$ ions of the DGDG 18:5/18:4 and 18:4/18:4 in the samples A, C and D showing quite different distribution of these two DGDGs. Thus, whereas in the sample A DGDG 18:4/18:4 is, as aforementioned, prevalent, two DGDGs (18:4/18:4 and 18:5/18:4) are present with different relative amounts both in sample C (Fig. 6b) and in sample D (Fig. 6c). Even if we have not yet a clear-cut evidence that DGDG 18:4/18:4 represents a specific signature of *Gs*-green species, the microscopic data (see biovolumes in Section 2) seem to support this working hypothesis. In fact, considering that 18:4 and 18:5 fatty acyl chains represent a reliable chemical signature of Dinophyta division [22–23] and that they are dominant in all the galactolipids of *Gs*-green extract (Table 2), it follows that the different ratio between the above-cited DGDGs as observed in ESI measurements (Fig. 6) must reflect a different distribution of dinoflagellate species. Thus, in the sample D, where the population of *Gs*-green species has been found in quite low amount (7%) by microscopic analysis, the relative amount (Fig. 6c) of DGDGs is exchanged, suggesting significant contribution from other dinoflagellate species. On this basis, we can use the outcome of our LC–ESI-MS measurements to establish that in sample C (Fig. 6b) the population of *Gs*-green is well represented. The fair agreement between DGDG distribution as estimated by our LC–ESI-MS data and the relative abundance of dinoflagellates as measured by microscopic analysis, suggests that our methodology could represent a powerful tool for the assessment of the composition of dinoflagellate assemblages at the species level.

3.4. Analysis of a shallow water microphytobenthos sample

Because of the mentioned famous reddening phenomenon, Lake Tovel has been studied from a variety of viewpoints, including a recent investigation on the depth-distribution of bottom living (=benthic) cyanobacteria and algae.

The methodology described in this paper can be applied also to freshwater microphytobenthos samples. Different pigments and lipids have been thus detected during our LC–MS analysis of samples obtained by extraction of cyanobacteria colonising stones taken at different depths in Lake Tovel. In the same chromatographic condition their abundant pigment markers, scytonemin and reduced scytonemin, can be promptly detected by positive-ion ESI-MS as $[M + Na]^+$ ions at *m*/*z* 567 and *m*/*z* 569, respectively. Scytonemin is a yellow-brown, lipid soluble dimeric pigment located in the extracellular polysaccharide sheath of some cyanobacteria [24]. Moreover, at a retention time between 22 and 35 min, besides galactolipids, an abundant sterol at $m/z = 423$, possibly the $[M + Na]^+$ ion of 3β-methoxycholest-5-ene, has been found. This sterol is believed to represent the most abundant steroid of the cyanobacterium *Scytonema* sp. [25].

4. Conclusions

We have developed a new HPLC–DAD-APIMS methodology that uses a single reversed-phase gradient separation and different MS experimental set-up (negative- or positive-ion mode, ESI or APCI ionisation, full scan or MS–MS). It is suitable both for the screening of pigments and for the detection of other interesting natural products from raw extracts of microalgae, such as MAAs and galactolipids, alkaloids and sterols. In particular, whereas the full structure characterization of MAAs requires a further LC–MS analysis with different mobile phase composition, that of galactolipids (both

DGDG and MGDG) can be defined at the level of molecular mass determination, composition and positional distribution of the *sn*-glycerol-bound fatty acyl chains. Our results show that galactolipids analysis seems to be a suitable tool for assessing new chemical markers with taxonomic significance even at the species level.

The methodology has been successfully applied to the monitoring both of the *Gs*-green enclosure-blooms induced by nutrient enrichment and of the natural phytoplankton community of Lake Tovel.

Acknowledgments

We thank dott. Giovanna Flaim for helpful discussions about the taxonomy of dinoflagellates of Lake Tovel. Work was financially supported by both MIUR2003 and UNIPAT-SALTO projects.

References

[1] J.W.G. Lund, C. Kipling, E.D. Le Cren, Hydrobiologia 11 (1958) 143.
[2] E. Rott, Schweiz, Z. Hydrol. 43 (1981) 34.
[3] H. Utermöhl, Mitt. Int. Verein. Limnol. 9 (1958) 1.
[4] D.F. Millie, H.W. Pearl, J.P. Hurley, Can. J. Fish. Aquat. Sci. 50 (1993) 2513.
[5] S.W. Jeffrey, M. Vesk, in: S.W. Jeffrey, R.F.C. Mantoura, S.W. Wright (Eds.), Phytoplankton Pigments in Oceanography, Unesco Publishing, Paris, 1997, p. 37.
[6] M.D. Mackey, D.J. Mackey, H.W. Higgins, S.W. Wright, Mar. Ecol. Prog. Ser. 144 (1996) 265.
[7] V.N. Karnaukhov, Comp. Biochem. Physiol. B 95 (1990) 1.
[8] R.B. van Breemen, Pure Appl. Chem. 69 (1997) 2061.
[9] H.D. Park, H. Hayashi, J. Phycol. 29 (1993) 435.
[10] A. Groniger, R.P. Sihna, M. Klisch, D.P. Häder, J. Photochem. Photobiol. B 58 (2000) 115.
[11] E.B. Örnólfsdóttir, J.L. Pinckney, J. Phycol. 39 (2003) 449.
[12] F. Pietra, Chem. Soc. Rev. 24 (1995) 65.
[13] F. Pietra, Biodiversity and Natural Product Diversity, Elsevier, Oxford, UK, 2002.
[14] M. Cantonati, M. Tardìo, M. Tolotti, F. Corradini, J. Limnol. 62 (2003) 79.
[15] R. Frassanito, G. Guella, G. Di Giuseppe, M. Cantonati, M. Tardìo, I. Mancini, F. Dini, Proceedings of 4th European Congress of Protistology and 10th European Conference on Ciliate Biology, San Benedetto del Tronto, Italy, 2003.
[16] Giovanna Flaim, personal communication.
[17] G. Guella, R. Frassanito, I. Mancini, Rapid Commun. Mass Spectrom. 17 (2003) 167.
[18] F. Cunningham, E. Gantt, Annu. Rev. Plant Physiol. Plant Mol. Biol. 49 (1998) 557.
[19] A.T. Banaszak, T.C. LaJeunesse, R.K. Trench, J. Exp. Mar. Biol. Ecol. 249 (2000) 219.
[20] K. Whitehead, D. Karenz, J.I. Hedges, Mar. Biol. 139 (2001) 1013.
[21] Y. Oshima, S. Yamada, K. Matsunaga, T. Moriya, Y. Ohizumi, J. Nat. Prod. 57 (1994) 534.
[22] C.C. Parrish, G. Bodennec, P. Gentien, Phytochemistry 47 (1998) 783.
[23] Y. Hiraga, K. Kaku, D. Omoda, K. Sugikara, H. Hosoya, M. Hino, J. Nat. Prod. 65 (2002) 1494.
[24] P.J. Proteau, W.H. Gerwick, F. Garcia-Pichel, R. Castenholtz, Experentia 49 (1993) 825.
[25] T. Řezanka, V.M. Dembitsky, J.V. Go, I. Dor, A. Prell, L. Hanuš, Folia Microbiol. 48 (2003) 357.